geologicaacta

Citation: Corradini C., Corriga M.G., Pondrelli M., Spalletta C., Zocchi C., Corradeti A., 2025. Record of a sea level drop in the lower Mississippian limestones near Passo di Monte Croce Carnico (Carnic Alps, Italy). Geologica Acta, 23.14, 1-15. DOI: 10.1344/GeologicaActa2025.14
Online ISSN: 1696-5728

Record of a sea level drop in the lower Mississippian limestones near Passo di Monte Croce Carnico (Carnic Alps, Italy).

Carlo Corradini[1] **Maria G. Corriga**[1] **Monica Pondrelli**[2] **Claudia Spalletta**[3]
Camilla Zocchi[1] **Amerigo Corradetti**[1]

[1.] **Dipartimento di Matematica, Informatica e Geoscienze, Università di Trieste**
via Weiss 2, 34128 Trieste (Italy). E-mail: Corradini E-mail: ccorradini@units.it;
Corriga E-mail: mariagiovanna.corriga@units.it; Zocchi E-mail: camilla.zocchi@studenti.units.it; Corradetti E-mail: amerigo.corradetti@units.it

[2.] **Dipartimento di Ingegneria e Geologia, Università d'Annunzio**
iale Pindaro 42, 65127 Pescara, Italy. E-mail: monica.pondrelli@unich.it

[3.] **Dipartimento di Scienze Geologiche, Biologiche e Ambientali, Alma Mater Studiorum-Università di Bologna**
via Zamboni 67, 40126 Bologna, Italy. E-mail:claudia.spalletta@unibo.it

ABSTRACT

The lower Carboniferous succession of the Carnic Alps represents the best-preserved example of such stratigraphic interval within the Alps, thus providing crucial insights for paleogeographic and paleoclimatic reconstructions. This research focuses on the combined biostratigraphic and sedimentological analyses of a stratigraphic section near Passo di Monte Croce Carnico (central Carnic Alps). The presence of two polygonal sedimentary structure-bearing levels suggests a sea level drop. Conodont biostratigraphy places these events within the lower part of the *Gnathodus* interregnum, correlating with the latest Tournaisian. These data, combined with insights from coeval sedimentary records within the Carnic Alps and from other basins worldwide, indicate that higher-frequency sea-level fluctuations, superimposed on an overall regressive trend, influenced the late Tournaisian evolution of the Carnic Basin.

KEYWORDS **Eustatic variations. Conodont biostratigraphy. Tournaisian. Carboniferous.**

INTRODUCTION

The Carnic Alps host one of the most complete and well-preserved Palaeozoic sequences globally, making them a key natural laboratory for studying Palaeozoic stratigraphy, relative sea-level changes and basin evolution in the western Paleotethys region. These rocks, spanning from the Middle Ordovician to the Permian, are litho- and bio-stratigraphically well featured and are subdivided into three unconformity-bounded major sequences: the Pre-Variscan Sequence (Dapingian?–Bashkirian), the Permo-Carboniferous Sequence (Moscovian–Kungurian), and the Alpine Sequence, which starts in the Late Permian and includes also younger rocks. For a summary refer to Corradini and Pondrelli (2021). The Pre-Variscan Sequence is particularly significant, because it represents the only (mainly) non-metamorphic succession of this age in the Alps, and, as a consequence, the reference area for obtaining

information on the basin evolution and the controls (local vs global) on its deposition. Furthermore, it provides critical insights into the paleogeographic evolution of the westernmost sectors of the Paleotethys Ocean northern continental margin, of which the Palaeozoic basin of the Carnic Alps was a part (*e.g.*, Von Raumer *et al.*, 2002).

These main sequences are bounded by major unconformities that are associated with important hiatuses related to the main stages of the tectonic evolution of the basin. In addition, additional minor hiatuses are also present within the sequences themselves, which are, mainly, disconformities or, less frequently, angular unconformities. One is located between the Ordovician and the Silurian, and it was associated with the Hirnantian glaciation (see the discussion in Corriga *et al.*, 2021). Another is located in the upper part of the sequence, where a distinctive facies transition occurs between the predominantly carbonate units of Devonian and early Carboniferous age and the siliciclastic rocks of the Variscan flysch marking the onset of synorogenic basin evolution (Corradini *et al.*, 2015b). Recent studies have also documented additional stratigraphic discontinuity surfaces, some of them related to intervals of subaerial exposure affecting at least parts of the basin, contributing to shedding light on its complex depositional history (*e.g.*, Corradini *et al.*, 2017b, 2024a; Pondrelli *et al.*, 2015, 2020). The Upper Devonian–lower Carboniferous part of the succession is particularly important because it records a major transition from the warm Middle Devonian greenhouse world to the cooler icehouse conditions of the late Carboniferous (Qie *et al.*, 2019, cum ref.).

Despite extensive research being carried out in the Carnic Alps, new evidence from Passo di Monte Croce Carnico (Fig. 1) highlights the occurrence of an outcrop showing a few metres thick conodont-bearing limestone section, hosting one bed bounded below and above by sedimentary surfaces showing evidence of postdepositional alteration, and whose conodont record allows a detailed correlation with other well-known sections in the area. By using an integrated approach of sedimentological observations, conodont biostratigraphy, high-resolution imaging, and regional geological context, these events are dated to the *Gnathodus* interregnum, and are followed by a resumption of limestone deposition

GEOLOGICAL SETTING

In the Passo di Monte Croce Carnico/Plockenpass area, rocks from Katian (Upper Ordovician) to Sepurkhovian (lower Carboniferous) are exposed, documenting a time interval of about 130 million years (Fig. 2). They belong to the Pre-Variscan sequence of the Carnic Alps (Corradini *et al.*, 2015b). The lithostratigraphy of this sequence was recently revised by Corradini and Suttner (2015), and thirty-six formations are now discriminated from the Middle Ordovician to the Early Pennsylvanian.

From the Ordovician to the Early Devonian, a relatively uniform sedimentation characterized the entire Carnic basin. At the beginning of the Devonian, the basin sedimentation began to differentiate and, in the proximal parts of the basin, large accumulations of fossil remains were deposited since the Emsian and formed extensive carbonate buildups. Reef proliferation expanded during the Middle Devonian, and persisted until the Frasnian. While reefs dominated the proximal areas, calm water sedimentation characterized the distal and deeper parts of the basin. In the slope depositional settings, thick bodies of gravity-driven reef detritus graded into deeper parts of the basin, and constitute the so-called "transitional sequence" (Pondrelli *et al.*, 2020). At the beginning of the Late Devonian, a combination of local tectonic movements and global sea-level variations led to the disappearance of the reefs (Corradini and Pondrelli, 2021). In the Carnic basin, the micritic limestones of the Pal Grande Formation were deposited in a relatively shallow sea, far from any emerged land. During the lower Carboniferous, the Carnic basin experienced significant tectonic activity (Spalletta and Venturini, 1988, 1995), leading to the drowning of some sectors of the basin, while other areas were uplifted, in some cases to emersion. Large submarine landslides resulted in the accumulation of breccias, conglomerates, sandstones, and pelites in the basin (Hochwipfel Fm.). The Variscan Orogeny interrupted the marine sedimentation during the late Bashkirian. For a detailed description of the Pre-Variscan Sequence, refer to Corradini and Suttner (2015) and Corradini and Pondrelli (2021, and references therein).

Compared to other areas of the Carnic Alps, the Variscan sequence is laterally uniform across the Monte Croce Carnico area. However, the lower part of the sequence is exposed exclusively on the Austrian side, whereas, in Italy, only rocks of Middle Devonian age or younger are exposed.

A prominent WNW trending fault (referred as 'main' fault in Figure 2) cuts through the area of Passo di Monte Croce Carnico and separates two successions that correspond to different parts of the Devonian basin (Fig. 2). To the South of the fault and a few km West of Passo di Monte Croce Carnico, Mt Creta di Collina represents the eastern termination of the largest Devonian reef of the Carnic Alps, represented by Mt Coglians massif. Here, the reef deposits of the Kellergrat Fm. (lower Givetian–Frasnian) are unconformably covered by the brachiopod-bearing breccia to mainly packstone of the Creta di Collina Fm. (upper Frasnian–lower Famennian). Then, the Creta di

FIGURE 1. A) Location map B) with a detailed topographic inset of Passo di Monte Croce Carnico (Plöckenpass). The studied section is marked with a black asterisk.

Collina Fm. pass gradually to the Pal Grande Fm. (lower Famennian–Visean).

To the North of the fault, the succession consists of the so-called 'transitional facies' units, which were deposited in slope-to-basin settings (Corradini and Pondrelli, 2021; Pondrelli *et al.*, 2020). In the study area, the succession starts with the massive rudstone deposits of the Cellon Fm. (lowermost Givetian), followed by the Freikofel Fm. (Givetian–Frasnian) and by the Pal Grande Fm. (uppermost Frasnian–Visean). All vertical transitions between these formations are gradual.

In both settings, the Pal Grande Fm. is unconformably overlain by the siliciclastic turbidites of the Hochwipfel Fm. (middle Visean–Bashkirian). Locally the unconformity is highlighted by the Plotta Fm. (?Tournaisian–?Visean), a unit mostly consisting of porous chert and limestone clasts interpreted as the product of the chemical and physical alteration processes related to an exposure event (Corradini *et al.*, 2017b; Pondrelli *et al.*, 2015; Schönlaub *et al.*, 1991). The Plotta Fm. is present in both parts of the fault, but it is thicker and widespread in the southern part of the study area. This disparity is probably due to a basin physiography inherited from the Middle Devonian evolution, which left the southern part of the study area in a shallower topographic position.

The studied outcrop exposes rock of the Pal Grande Formation (Spalletta *et al.*, 2015a). This unit consists of

grey fossiliferous mudstone and wackestone sedimented in a pelagic environment that was far from land but not particularly deep. At places, the colour turns reddish, mainly in the lower part of the unit. The age spans from the Frasnian (FZ 9; Joachimski *et al.*, 1994) to the Visean (*Gn. texanus* Zone; Perri and Spalletta, 1998d). However, in different sectors of the Carnic Alps, some biozones are at place missing. These hiatuses are evidenced by minor unconformities or paraconformities, suggesting local subaerial exposures of parts of the basin.

PREVIOUS RESEARCH IN THE AREA

The area around Passo di Monte Croce Carnico has been extensively explored by geologists since the 19th century, and tens of papers have been published on various aspects of the geology, palaeontology, and stratigraphy of the area. A recent geological map of the central sector of the Carnic Alps, including the Passo di Monte Croce Carnico area, was published by Pondrelli *et al.* (2020).

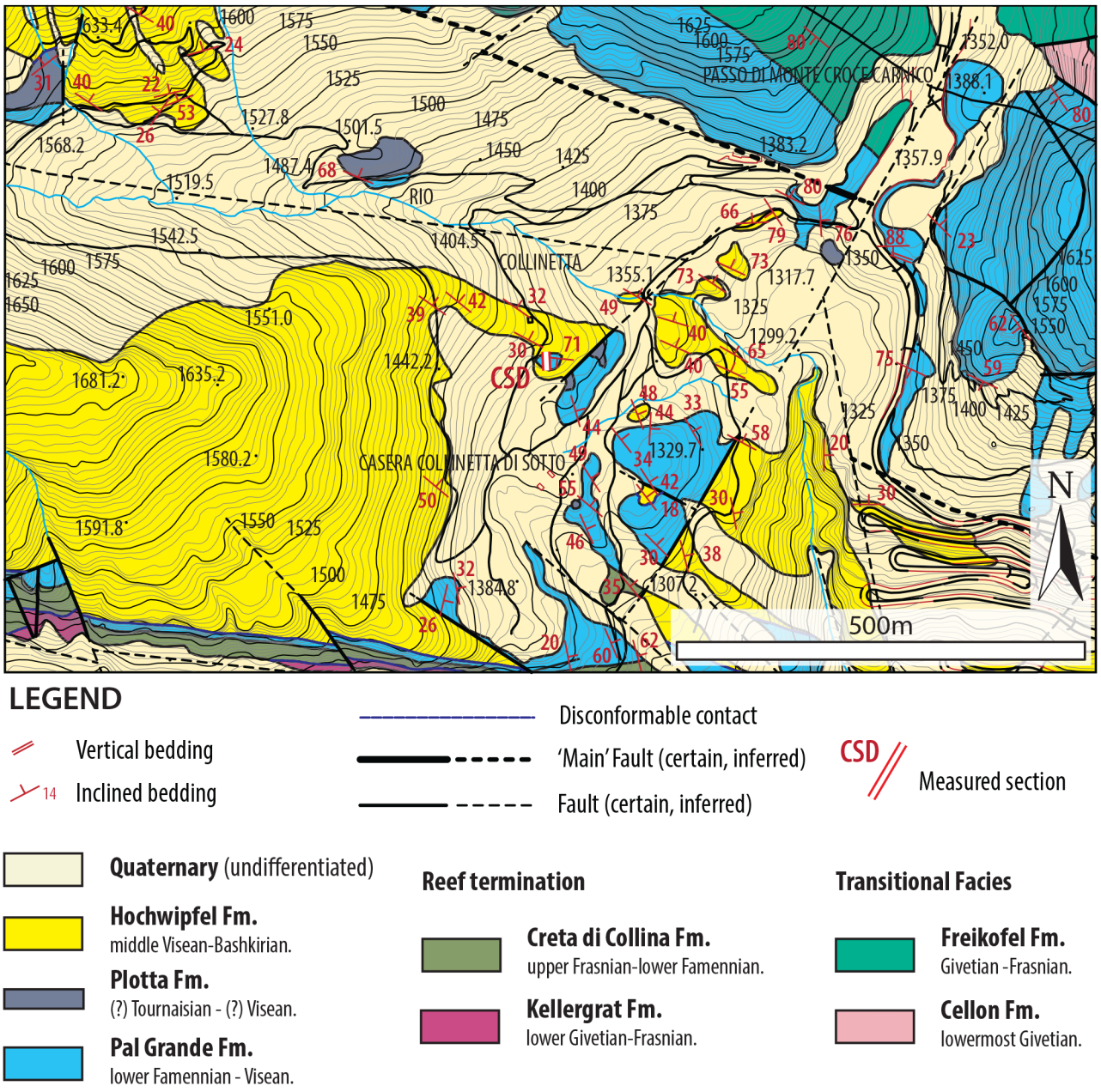

FIGURE 2. Geological map of the area around Passo di Monte Croce Carnico.

A few stratigraphic sections in the area serve as reference sections for global studies. For example, the Cellon section is a reference section for the uppermost Ordovician and the Silurian (Corradini *et al.*, 2015a and references therein; Corriga *et al.*, 2016; Walliser, 1964) and the Grüne Schneid section for the Devonian/Carboniferous boundary (Schönlaub *et al.*, 1988; Spalletta *et al.*, 2021 and references therein). While a complete list of publications on this part of the Carnic Alps would be too extensive, here we focus on research conducted in the near proximity to Casera Collinetta di Sotto area, where the present study has been performed.

Gedik (1974) illustrated the Famennian and Carboniferous conodont fauna of several localities in the Passo di Monte Croce Carnico area. Later, Perri and Spalletta (1998a, b, c) and Corradini and Pondrelli (2021) described the conodont biostratigraphy of several Famennian to Visean limestone section of the Pal Grande Fm., which are located to a few tens of metres to the south-east of the Casera Collinetta di Sotto D new section here studied (see below), which are hereafter listed in stratigraphic order. The Casera Collinetta di Sotto C section (Perri and Spalletta, 1998a) exposes about 18.5m of Famennian limestones dated to the *Palmatolepis marginifera utahensis* Zone. The Casera Collinetta di Sotto B section (Perri and Spalletta, 1998b) is more than 30m thick and exposes rocks from the *Pa. m. utahensis* to the *Palmatolepis gracilis manca* Zone.

The Casera Collinetta di Sotto A section (Corradini and Pondrelli, 2021; Perri and Spalletta, 1998c) exposes about 15m of grey to pinkish micritic limestones, unconformably capped by a silcrete level attributed to the Plotta Fm. Conodonts from the limestone beds allow to discriminate six Famennian Zones from the *Pseudopolygnathus granulosus* to the *Bispathodus ultimus*, the upper Tournaisian *Scaliognathus anchoralis* Zone, and the *Gnathodus* interregnum which spans the Tournaisian/Visean boundary interval. The top of the Famennian and most of the Tournaisian are missing in the carbonate succession, with a hiatus of at least 10Ma, evidenced in the field by a 30cm thick mineralized horizon.

NOTES ON UPPER TOURNAISIAN/LOWER VISEAN CONODONT BIOSTRATIGRAPHY

In comparison to the lower and middle Tournaisian conodont zonations (Lane *et al.*, 1980; Sandberg *et al.*, 1982), which are still in use with some modifications only in the lower part (Corradini *et al.*, 2017a; Kaiser *et al.*, 2009), the upper Tournaisian scheme is less stable, and no standard, global, zonation has yet been established.

Barrick *et al.* (2022) showed four major regional zonations in use in the Mississippian: the European deep-water, the standard Russian, the South China, and the North American Midcontinent zonations. The taxa used in these zonal schemes are essentially the same, but in each region the succession of species and reported ranges differ slightly, which has led to different zonations. The same approach is followed by Corradini *et al.* (2024b) in their review on global conodont biostratigraphy.

For a long time the *anchoralis-latus* Zone was considered as the youngest zone of the Tournaisian, followed around the base of the Visean by a *texanus* Zone or a *homopunctatus* Zone (*i.e.*: Groessens, 1974; Higgins and Austin, 1985; Lane *et al.*, 1980; Perret and Delvolve, 1994; Ziegler and Lane, 1987), depending on the geographic areas.

After the redefinition of the base of the Visean by the first occurrence of the foraminifer *Eoparastaffella simplex* (Devuyst *et al.*, 2003), ratified in 2008 by the International Commission on Stratigraphy (ICS), the conodont zonation had to be recalibrated. The event that better approximates the Tournaisian/Visean boundary is the first occurrence of *Pseudognathodus homopunctatus* (Ziegler, 1960), which enters slightly above, whereas the last representatives of *Scaliognathus anchoralis* Branson and Mehl, 1941 became extinct well below the boundary. The interval between the LAD of *Sc. anchoralis* and the FAD of *Gn. homopunctatus* has been named differently by various authors (*i.e.*: Bábek *et al.*, 2010; Devuyst and Kalvoda, 2007; Devuyst *et al.*, 2003) and is characterized by the presence of several long-ranging species of *Gnathodus*.

In the Carnic Alps, Schönlaub *et al.* (1991) used the old concept of the *anchoralis-latus* Zone, extended to all the upper Tournaisian, and Perri and Spalletta (1998d) proposed a *texanus-homopunctatus* Zone immediately following the *anchoralis-latus* Zone for the base of the Visean. In their sections at the Tournaisian/Visean boundary, Perri and Spalletta (1998d) recognized a stratigraphic interval characterized by "a monotonous, long-ranging gnathodid fauna" between the last appearance of the scaliognathids and the first appearance of *Pseudognathodus homopunctatus*.

In this paper, we follow the scheme suggested by Devuyst and Kalvoda (2007), as adopted by Corradini *et al.* (2017b), with the *anchoralis* Zone in the upper Tournaisian and a *Gnathodus* interregnum across the Tournaisian/Visean boundary, followed by an *homopunctatus* Zone in the lower Visean.

MATERIAL AND METHODS

Sample preparation and study were undertaken at the Department of Mathematics, Informatics and Geosciences

of the University of Trieste, Italy. Conodonts were extracted from limestone samples by conventional formic acid technique at a 4% concentration. Conodont elements were extracted by hand picking from unseparated residue under binocular microscopes. The whole fauna is stored in the micropalaeontological collections of the Department of Mathematics, Informatics and Geosciences of Trieste University.

Selected conodonts were photographed with the photo stacking method described by Zocchi and Corradini (2024) using a Nikon D7100 camera equipped with Mitakon 20mm f/2 4.5X super macro lens. Other specimens were photographed by a Scanning Electron Microscope (SEM) JEOL JSM-6010PLUS/LA at the Department of Chemical and Geological Sciences of the University of Modena and Reggio Emilia, Italy.

A Virtual Outcrop Model (VOM; Xu *et al.*, 2000) of the studied section, showing the evidence of sub-aerial exposure, was generated using the Structure from Motion-Multi View Stereo (SfM-MVS) photogrammetry technique (*e.g.*, Arbués *et al.*, 2012; Favalli *et al.*, 2012) from a set of 234 (3968x2976 pixels) photographs collected using a DJI Spark™ UAV (Unmanned Aerial Vehicle). The VOM was created following the well-established workflow in Agisoft Metashape software (*e.g.*, Carrivick *et al.*, 2016; Corradetti *et al.*, 2022). It was then used to produce a bedding-perpendicular, orthorectified view of the observed polygonal features, enabling quantitative analysis without perspective distortion. Additionally, the VOM serves to digitally preserve the outcrop, promote digital accessibility and enhance reproducibility of the study, as sampling locations are clearly marked within the model (Burnham *et al.*, 2022; Cawood and Bond, 2019), available at the link provided in the next section.

THE CASERA COLLINETTA DI SOTTO D (CSD) SECTION

The Casera Collinetta di Sotto D section is exposed about 600m Southwest of Passo di Monte Croce Carnico, at coordinates 46°36'02.6" N, 12°56'07.7" E and altitude of 1415m (Zocchi, 2022). Here about 7m of massive grey limestones of the Pal Grande Formation are exposed, organized in thick beds dipping roughly 70° to the south (Figs. 3-4), and entirely bounded by pelites and sandstones of the Hochwipfel Formation. The limestones represent an olistolith of Pal Grande Formation material slid within the Hochwipfel Formation.

The section consists of gray mudstone and wackestone. Macrofossils are rare, and only a few ammonoids are observable in the field (Fig. 3C-E). In general, they are relatively abundant in the bed of sample CSD 3 (Fig. 3C), whereas isolated specimens are present in the central part of the section (Fig. 3D-E).

The original bedding is mostly concealed by pressure-solution processes. However, two bedding surfaces, about 20cm apart in the central part of the section, are distinguished by decimetre-scale polygonal structures affecting the limestone. These features are fractures filled with mudstone and siltstone, and are well visible because they are more resistant to weathering and erosion compared to the limestone host rock (Fig. 3B, F). These structures exhibit a polygonal shape similar throughout the two beds. Their morphometric parameters have been derived from a population of 50 polygons using an orthorectified image not subject to perspective deformation (Fig. 3G). The polygons show a maximum dimension ranging from 5 to 12cm, with most of them being around 7cm. The length-to-height ratio in about 70% of the cases ranges between values of 0.83 and 1.23, meaning that most of the polygons are fairly regular. A significant percentage of polygons, though, shows elongated shapes. Despite the post-depositional deformation, where the structures are visible in lateral view, they show a V-shaped downward termination. Such sedimentary structures might, in principle, represent shrinkage, either desiccation or syneresis cracks, or microbially induced structures, or be related to bioturbation (see discussion below).

The microfacies is represented by a biomicritic packstone/wackestone with high content of fossil debris of goniatites, trilobites, ostracods and possible radiolarians, among others (Fig. 5). A low-resolution version of the VOM (~2.3M triangles and 8192x8192 pixels), showing the exact positions of the collected rock samples, is available in the Sketchfab public repository at https://skfb.ly/oMNM7.

Conodont data

Six conodont samples were collected from the CSD section and processed with the conventional formic acid technique. About 10.6kg of rocks yielded about 550 conodont elements (Tab. 1). About one fourth of the association is represented by ramiform elements. The state of preservation is generally quite good, even if some elements are broken. Conodont colour is dark brown, corresponding to a Colour Alteration Index (CAI) of 4 (Fig. 6). The abundance is variable from 178 elements/kg (sample CSD 1) to 16 (sample CSD 0), with an average of 56 elements/kg (Tab. 1).

Twelve species belonging to six genera (*Bispathodus*, *Gnathodus*, *Lochreia*, *Protognathodus*, *Pseudopolygnathus* and *Scaliognathus*) were identified (Figs. 6-7; Tab. 1). Genus *Gnathodus* is by long

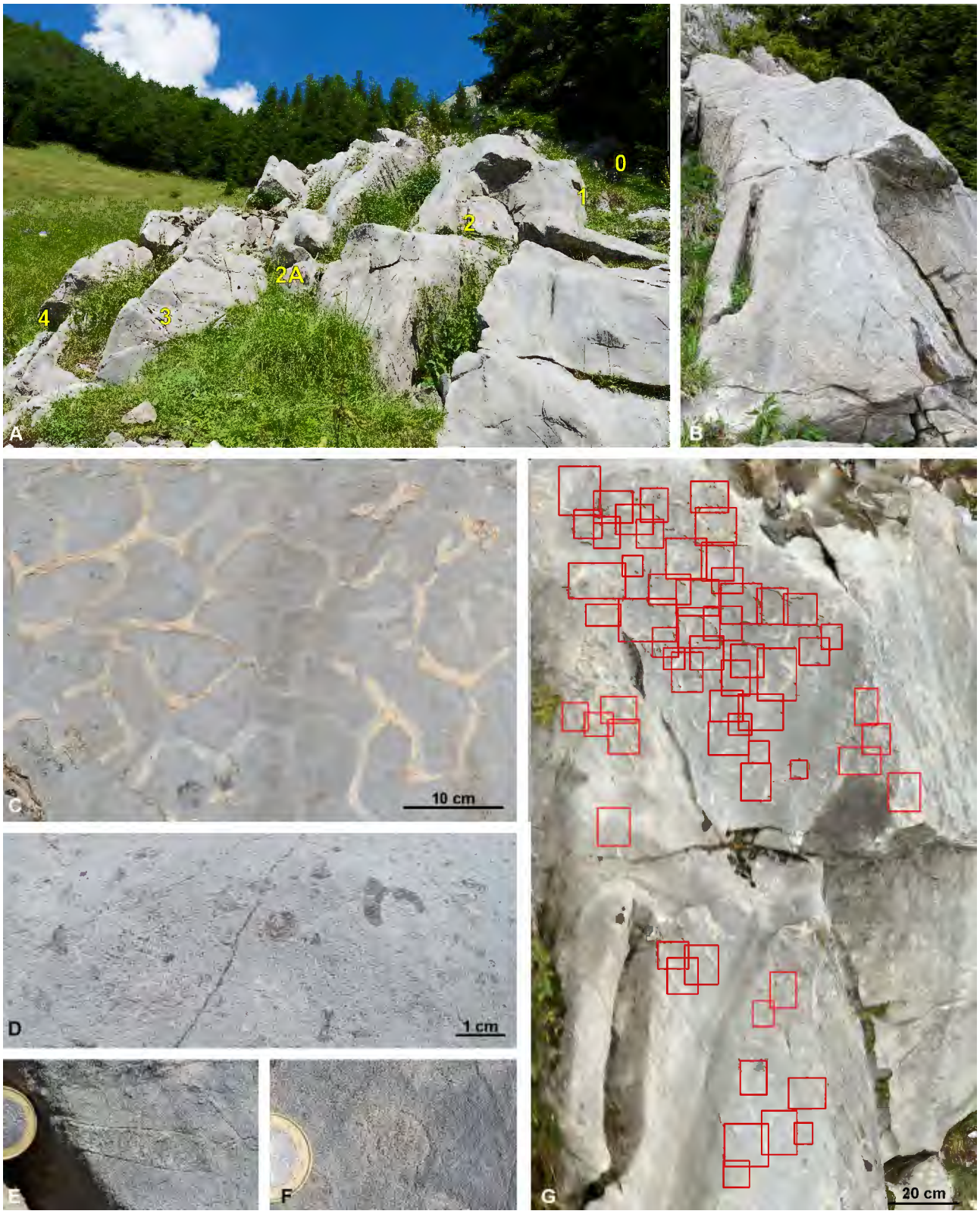

FIGURE 3. Selected views of the CSD section. A) View of the section with the position of the samples highlighted in yellow. B) View of the bedding plane showing polygonal structures. C) Close-up view of a bed rich in ammonoid remnants. D) Longitudinal section of an ammonoid. E) Transversal view of an ammonoid. F) Detail of the surface with polygonal structures. G) Orthorectified image showing the recognized polygonal structures enclosed within red-bordered rectangles. These shapes have been used to derive the length and height of different features for morphometric analysis.

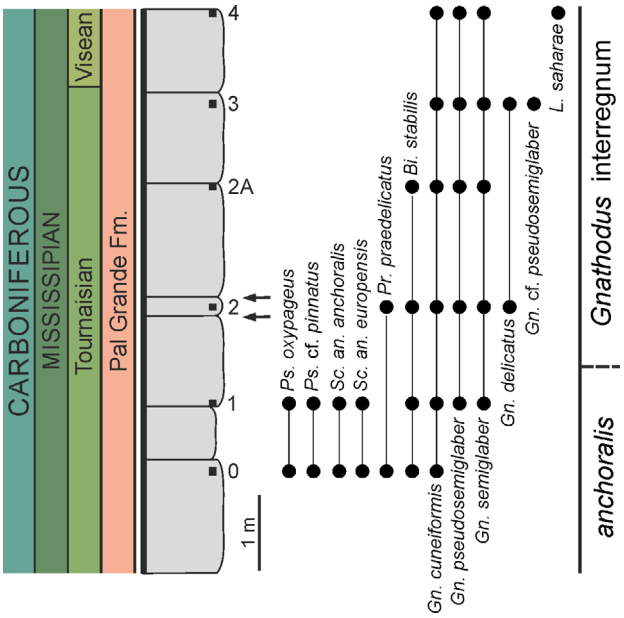

FIGURE 4. Chronostratigraphy (System, Series, Stage), lithostratigraphy, stratigraphic column, conodont samples, distribution of conodonts, and biostratigraphy of the Casera Collinetta di Sotto D (CSD) section. The arrows indicate the two levels with polygonal structures. Abbreviations: *Bi.* = *Bispathodus*, *Gn.* = *Gnathodus*, *L.* = *Lochriea*, *Pr.* = *Protognathodus*, *Ps.* = *Pseudopolygnathus*, *Sc.* = *Scaliognathus*.

the more represented in all samples, and represents more than 90% of the fauna. The two species *Gn. pseudosemiglaber* Thompson and Fellows, 1970 and *Gn. semiglaber* Bischoff, 1957 represent the 26% each. *Pseudopolygnathus* and *Scaliognathus* are present only in the lowermost part of the section (samples CSD 0 and CSD 1), where rare elements of *Ps. oxypageus* Lane, Sandberg and Ziegler, 1980, *Ps. pinnatus* Voges, 1959, *Sc. anchoralis anchoralis* Branson and Mehl, 1941 and *Sc. an. europensis* Lane and Ziegler, 1983 occur.

Biostratigraphy

Two biozones at the Tournaisian/Visean boundary are discriminated in the Casera Collinetta di Sotto D section (Fig. 4):

Scaliognathus anchoralis Zone

This Zone corresponds to the total range of *Scaliognathus an. anchoralis* and *Sc. an. europensis*. It has been discriminated in the lower part of the section (sample CSD 0-1) by the presence of both markers. *Gnathodus semiglaber* and *Gn. pseudosemiglaber* are present in the upper part of the Zone. Genus *Pseudopolygnathus* is present only in this part of the section.

Gnathodus interregnum

This Zone is the interval between the LAD of the subspecies of *Scaliognathus anchoralis* and the FAD of *Pseudognathodus homopunctatus*, and spans the Tournaisian/Visean boundary. It has been discriminated in the upper part of the Casera Collinetta di Sotto D section. The lower boundary occurs above sample CSD 1, where both *Scaliognathus an. anchoralis* and *Sc. an. europensis* have their last occurrence, and the Zone reaches the top of the section. It is important to note that the occurrence of one small element of *Lochreia saharae* Nemyrovska,

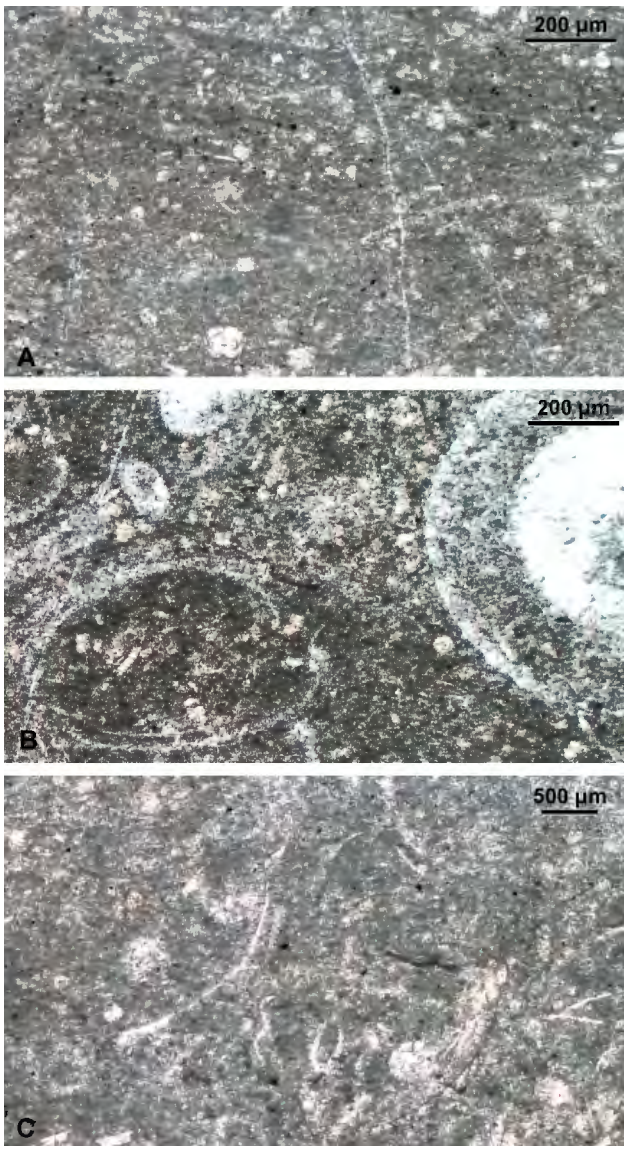

FIGURE 5. Microfacies of the Pal Grande Fm. in the CSD section. A) Biomicritic packstone, Sample CSD 0. B) Biomicritic packstone with large goniatite and brachiopod shells, sample CSD 2. C) Biomicritic packstone/wackestone, sample CSD 2A.

Perret-Mirouse and Weyant, 2006 in sample CSD 4 indicates that the upper part of the section already has a Visean age.

DISCUSSION

The polygonal sedimentary structures represent the most distinctive features in an otherwise homogeneous deposit. The genetic interpretation of such features, if not associated with other sedimentary structures or deposits, can be controversial due to the equifinality of this polygonal morphology. In particular, the genesis of these structures might reflect processes like desiccation related to exposure phases, biogenic activity (bioturbation), associated with microbial fauna (microbially induced sedimentary structures; *e.g.*, El Kabouri *et al.*, 2023), synaeresis cracks (Pratt, 1998), or seismites, following mud shrinkage and sediment injection related to earthquakes (Pratt and Ponce, 2019; Pratt *et al.*, 2024). Nonetheless, several considerations can be put forward.

Post-depositional deformation hampers the detailed characterization of the morphometric parameters in three dimensions. However, the overall shape and scale of the polygons appear too regular to suggest injection from the subsurface. Our data does not allow to rule out formation as synaeresis cracks or seismites, but this possibility seems less likely. Moreover, there is no evidence of microbialites in these deposits, unlike those observed in other parts of the Carnic Alps (*e.g.*, Farabegoli *et al.*, 2023), so that the hypothesis of a genesis related to microbial activity appears unlikely.

The polygonal geometry observed at the top of beds 1 and 2 may have formed as mud cracks resulting from desiccation after exposure events. The length-to-height ratio of individual features, as observed in the undeformed orthomosaic (Fig. 3G), is mostly around 1, and this regular pattern, along with their fairly similar dimensions, supports this interpretation. However, many of the angles shaping the polygons are rounded, which is inconsistent with this hypothesis. Additionally, a minority

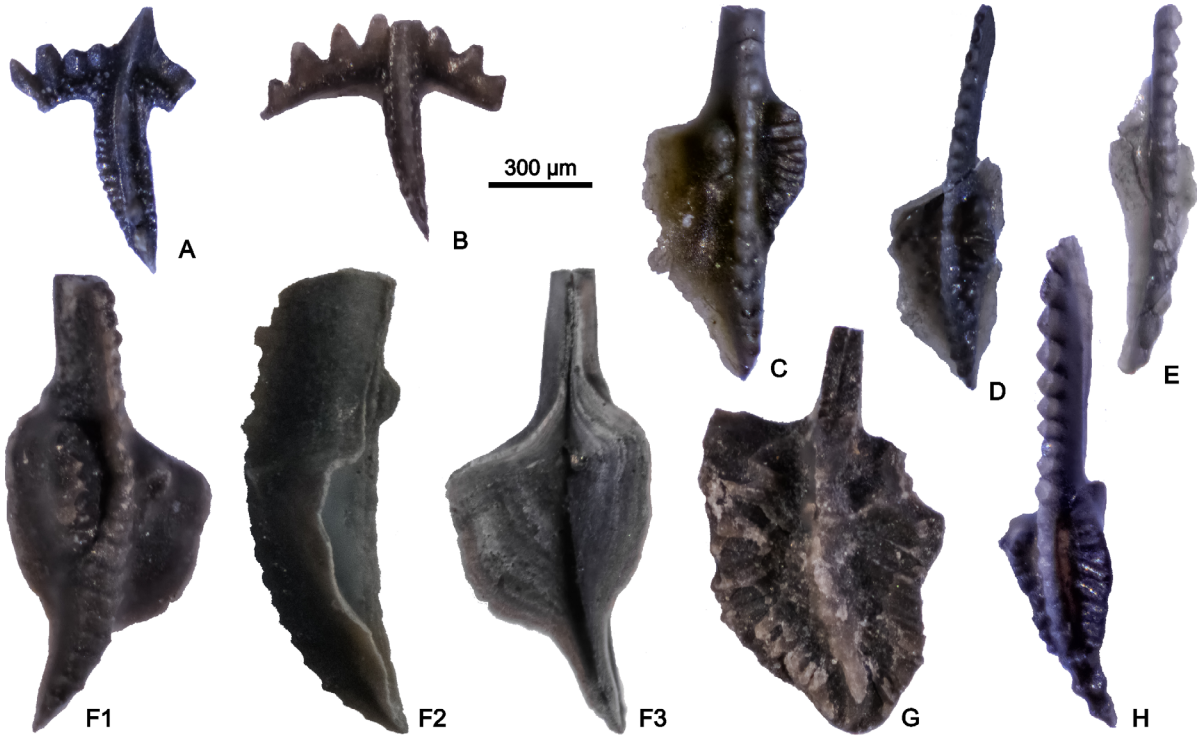

FIGURE 6. Selected conodonts photographed using the photo stacking method. A) *Scaliognathus anchoralis anchoralis* Branson and Mehl, 1941; upper view of P1 element; sample CSD 0. B) *Scaliognathus anchoralis europensis* Lane and Ziegler, 1983; upper view of P1 element; sample CSD 1. C) *Gnathodus pseudosemiglaber* Thompson and Fellows, 1970; upper view of P1 element; sample CSD 2. D) *Gnathodus cuneiformis* Mehl and Thomas, 1947; upper view of P1 element; sample CSD 2. E) *Bispathodus stabilis stabilis* (Branson and Mehl, 1934); upper view of P1 element; sample CSD 2. F) *Gnathodus semiglaber* Bischoff, 1957; upper (F1), lateral (F2) and lower (F3) views of P1 element; sample CSD 3. G) *Pseudopolygnathus pinnatus* Voges, 1959; upper view of P1 element; sample CSD 0. H) *Gnathodus cuneiformis* Mehl and Thomas, 1947; upper view of P1 element; sample CSD 1.

of the polygonal structures exhibit an elongated pattern, further complicating this interpretation. Moreover, no other sedimentary structures associated with subaerial exposure (*e.g.*, tepee, caliche) have been found, making it impossible to unambiguously confirm the occurrence of subaerial exposure. The morphometric parameters of the polygonal pattern may also be consistent with formation by trace fossils, possibly *Thalassinoides* (*e.g.*, Liu *et al.*, 2024; Yanin and Baraboshkin, 2013), although the forms appear more interconnected than is typical for this ichnogenus. Also, *Thalassinoides* is made by burrowers, whilst the polygonal structures in the CSD section are placed on

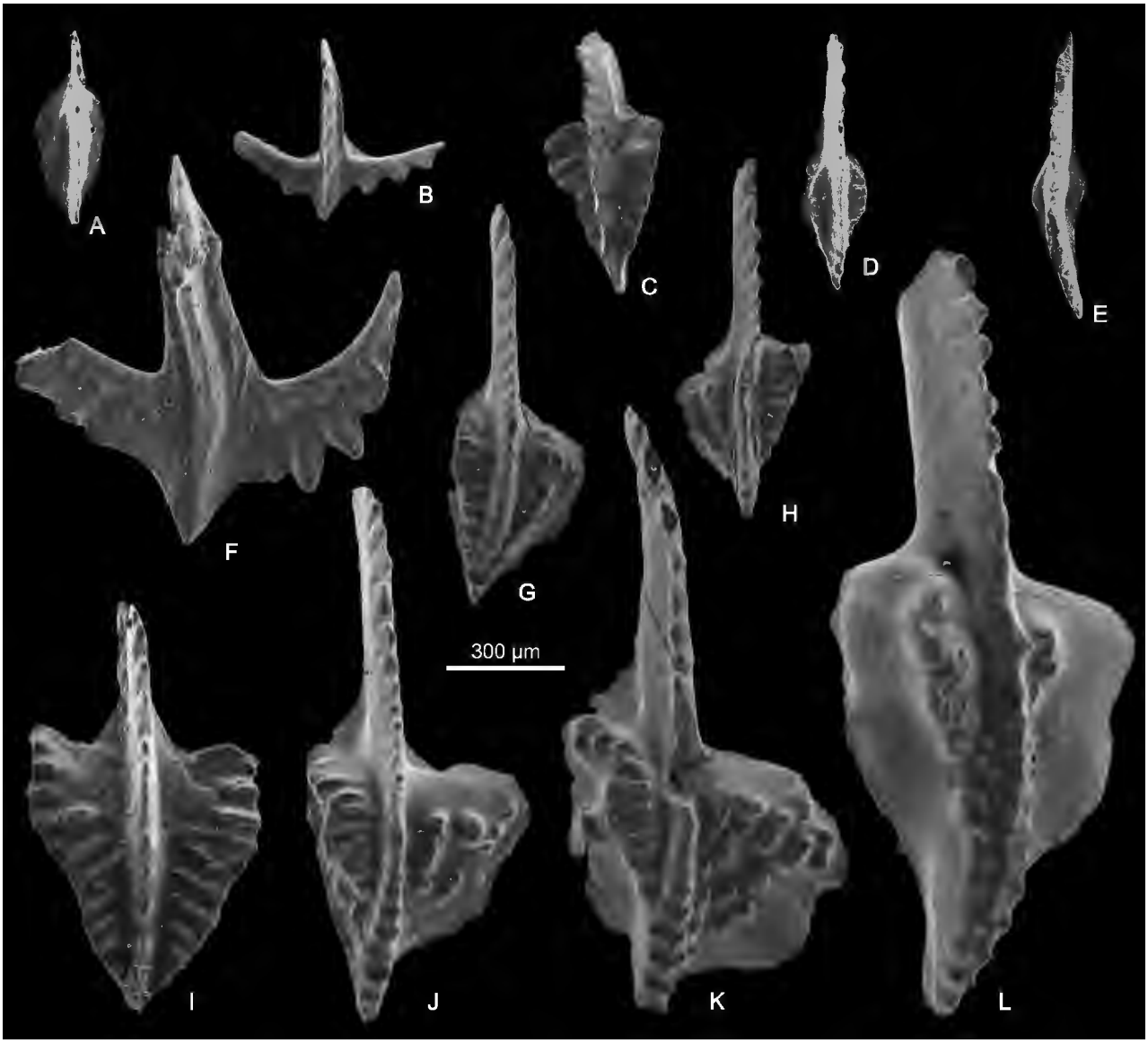

FIGURE 7. SEM photos of selected conodonts.
A) *Lochreia saharae* Nemyrovska, Perret-Mirouse and Weyant, 2006; upper view of P1 element; sample CSD 4. B) *Scaliognathus anchoralis europensis* Lane and Ziegler, 1983; upper view of P1 element; sample CSD 0. C) *Pseudopolygnathus oxypageus* Lane, Sandberg and Ziegler, 1980; upper view of P1 element; sample CSD 1. D) *Gnathodus cuneiformis* Mehl and Thomas, 1947; upper view of P1 element; sample CSD 4. E) *Bispathodus stabilis stabilis* (Branson and Mehl, 1934); upper view of P1 element; sample CSD 2A. F) *Scaliognathus anchoralis anchoralis* Branson and Mehl, 1941; upper view of P1 element; sample CSD 1. G) *Gnathodus cuneiformis* Mehl and Thomas, 1947; upper view of P1 element; sample CSD 2. H) *Gnathodus semiglaber* Bischoff, 1957; upper view of P1 element; sample CSD 3. I) *Pseudopolygnathus cf. pinnatus* Voges, 1959; upper view of P1 element; sample CSD 1. J) *Gnathodus cf. pseudosemiglaber* Thompson and Fellows, 1970; upper view of P1 element; sample CSD 3. K) *Gnathodus cf. pseudosemiglaber* Thompson and Fellows, 1970; upper view of P1 element; sample CSD 3. L) *Gnathodus pseudosemiglaber* Thompson and Fellows, 1970; upper view of P1 element; sample CSD 3.

bedding planes. Due to the limited size of the outcropping area containing polygonal features and the effects of post-depositional deformation (CAI= 4.3, suggestive of anchizone conditions; Brime *et al.*, 2008), it is not possible to definitively support or rule out either hypothesis.

Desiccation cracks would indicate subaerial exposure, while the two levels of bioturbation may suggest the formation of a hardground settling associated with a decline in carbonate factory production, leading to condensed sedimentation. Alternatively, a transgressive phase with more oxygenated conditions may have promoted bioturbation. However, this transgressive scenario is not supported by the rock record, which shows neither a revival of the carbonate factory nor a landward or deepening facies migration at the basin scale. Therefore, both scenarios point to a sea-level drop.

A sea-level drop is further supported by global data. In the late Tournaisian a prominent global regression took place, followed by a sharp transgression within the early Visean. The sequence boundary occurred above the last occurrence of *Sc. a. anchoralis* (Babek *et al.*, 2010) and is more or less coincident with the stage boundary. In several regions where the Tournaisian sequences primarily consist of shallow-water sediments, evidence of subaerial exposure, such as karst surfaces in China (Hance *et al.*, 1997), karst and facies variations in northern continental Europe and British Isles (Babek *et al.*, 2010; Hance *et al.*, 2001; Herbig, 2016; Poty, 2016), and evaporite deposition in North America (Petty 2010), have been documented.

In the Carnic Alps the Tournaisian depositional setting is an open sea, where pelagic, though not deep, limestones sedimented. The area was far from any land and, therefore, the global regression did not result in facies changes (Corradini *et al.*, 2017b). Nevertheless, evidence of subaerial exposures is documented in the uppermost Tournaisian and across the Tournaisian/Visean boundary in various parts of the Carnic Alps. Schönlaub *et al.* (1991) postulated a widespread emersion in the uppermost Tournaisian. Their evidence is based on the mostly disconformable contact between the Pal Grande Formation limestone and the Hochwipfel Formation, often emphasized by the presence of a cherty lentiform horizon which at places includes regolith facies (Plotta Fm., Spalletta *et al.*, 2015b). The available conodont data indicate an age for this exposure within the *anchoralis-latus* Zone" (Schönlaub *et al.*, 1991, p. 93). Beside this regolith, in some localities, a breccia horizon consisting of limestone clasts, supported by an ochraceous pelitic matrix, occurs at the top of the limestones at the disconformity surface that separates the limestones from the overlying flysch deposits. The age of the clasts is comprised between the age of the topmost underlying limestone and the *anchoralis-latus* conodont Zone. The breccia was interpreted by Schönlaub *et al.* (1991) as a dissolution collapse breccia. Also, fissures and caves are present in the uppermost part of the limestones. Based on these data, Schönlaub *et al.* (1991) concluded that the Carnic Alps were interested by a widespread emersion during the *anchoralis-latus* conodont Zone (upper Tournaisian), followed by sudden deepening that generated the deposition of the Hochwipfel Fm.

Corradini *et al.* (2017b) documented a subaerial exposure in the Rio Sglirs area (near Cason di Lanza pass) by the occurrence of a palaeodoline and a loose mud-cracks-bearing block. The authors dated the exposure to the upper part of the *Sc. an. anchoralis* Zone. Pondrelli *et al.* (2015) proposed an exposure surface around the Tournaisian/Visean boundary in the Mt. Pizzul area, South of Cason di Lanza Pass. These two exposures are not coeval: this might reflect a series of higher-frequency eustatic cycles within the late Tournaisian, and/or the influence of local tectonics, which caused a subaerial exposure of at least parts of the area. This preceded a possibly more widespread emersion near the Tournaisian–Visean boundary, associated with a global sea-level low stand.

The importance of local tectonics was proposed by Vai (1998, and references therein) who interpret the occurrence of sedimentary dykes and breccias as related to extensional tectonic activity in the general geodynamic context of a deepening of the Carnic Basin and by Spalletta and Venturini (1995), who proposed a transtensional-transpressional regime that fragmented the basin into fault-bounded blocks so that parts of these blocks were locally uplifted to subaerial exposure, whereas other blocks underwent rapid deepening and the carbonatic pelagic sedimentation persisted to the deposition of radiolarian chert below the CCD (Spalletta and Venturini, 1988; Venturini and Spalletta, 1998).

While it is difficult to distinguish between the local tectonic and eustatic controls, the different exposure surfaces documented in the Tournaisian of the Carnic Alps align with the high frequency 4th order eustatic variations documented in the Tournaisian and in the Visean in northern Europe (Poty, 2016; Herbig, 2016), within a 3rd order sequence boundary more or less coincident with the stage boundary, or just below (Babek *et al.*, 2010).

The two mud-cracks-bearing potentially exposure surfaces in the CSD section are just above and just below sample CSD 2, and are dated to the lower part of the *Gnathodus* interregnum: their age correspond with the maximum regression of the 3rd order sequence boundary, and this suggest an eustatic control on their formation.

CONCLUSION

New data from the Casera Collinetta di Sotto D section near Passo di Monte Croce Carnico (Carnic Alps) provide evidence for a sea level drop event during the latest Tournaisian, within the *Gnathodus* interregnum Zone. This interpretation is supported by the presence of polygonal sedimentary structures and by the local and global geological context. Although alternative explanations such as synaeresis cracks, seismites, or microbially induced sedimentary structures cannot be entirely ruled out, polygonal sedimentary structures are morphologically consistent with a genesis either as desiccation cracks or by bioturbation. Such interpretation would suggest either a subaerial exposure or condensed sedimentation in a context of reduced carbonate factory production. Both settings are suggestive of sea level drop conditions, specifically indicating at least two episodes of high-frequency eustatic fluctuations near the Tournaisian/Visean boundary. These findings are consistent with similar sea-level variations documented in other parts of the Carnic Alps and worldwide, including China, northern Europe, the British Isles, and North America and support the interpretation of a global regression during the latest Tournaisian, followed by a transgression in the lower Visean.

ACKNOWLEDGMENTS

Annalisa Ferretti (Modena and Reggio Emilia University) helped in taking SEM-microphotographs at Modena University, and Stefano Devoto (Trieste) in the field. The manuscript was improved thanks to the comments by Agustín Martín-Algarra, Rosario Rodríguez-Cañero and Gustavo Voldman, and the editor Telm Bover-Arnal.

This research was performed within the framework and with the financial support of the European Community – Next Generation EU, Italian Ministry of University and Research, CUP J53D23002950006, PRIN 2022 Project n. 2022ZH5RWP "DEtailing thE Palaeogeography of Southern PAlaeoeurope by meanS of biosTratigraphic correlation and basin development in the Palaeozoic to early Mesozoic time-frame: case histories from the Italian record (DEEP PAST)"

REFERENCES

Arbués, P., García-Sellés, D., Granado, P., López-Blanco, M., Muñoz, J.A., 2012. A Method for Producing Photorealistic Digital Outcrop Models. ???? .74th EAGE Conference and Exhibition, ????, Pag????. Last accessed: ????. Website: http://www.earthdoc.org/publication/publicationdetails/?publication=59010

Bábek, O., Kalvoda, J., Aretz, M., Cossey, P.J., Devuyst, F.X., Herbig, H.J., Sevastopulo, G., 2010. The correlation potential of magnetic susceptibility and outcrop gamma-ray logs at Tournaisian-Viséan boundary sections in western Europe. Geologica Belgica, 13, 291-308.

Barrick, J.E., Alekseev, A.S., Blanco-Ferrera, S., Goreva, N.V., Hu, K., Lambert, L.L., Nemyrovska, T.I., Qi, Y., Ritter, S.M., Sanz-Lopez, J., 2022. Carboniferous conodont biostratigraphy. In: Lucas, S.G., Schneider, J.W., Wang, X., Nikolaeva, S. (eds.). The Carboniferous Timescale. Geological Society of London, Special Publication, 512, 695-768. DOI: https://doi.org/10.1144/SP512-2020-38

Bischoff, G., 1957. Die Conodonten-Stratigraphie des rhenoherzynischen Unterkarbons mit Berücksichtigung der Wocklumeria-Stufe und der Devon/Karbon-Grenze. Abhandlungen des Hessisches Landesamtes für Bodenforschung, 19, 1-64.

Branson, E.B., Mehl, M.G., 1934. Conodonts from the Grassy Creek shale of Missouri. Missouri University Studies, 8, 171-259.

Branson, E.B., Mehl, M.G., 1941. New and little known Carboniferous conodont genera. Journal of Palaeontology, 15, 97-106.

Brime, C., Perri, M.C., Pondrelli, M., Spalletta, C., & Venturini, C., 2008. Polyphase metamorphism in the eastern Carnic Alps (N Italy–S Austria): clay minerals and conodont Colour Alteration Index evidence. International Journal of Earth Sciences, 97, 1213-1229. DOI: https://doi.org/10.1007/s00531-007-0218-7

Burnham, B., Bond, C., Flaig, P., van der Kolk, D., Hodgetts, D., 2022. Outcrop conservation: Promoting accessibility, inclusivity, and reproducibility through digital preservation. The Sedimentary Record, 20(1), 5-14. DOI: https://doi.org/10.2110/sedred.2022.1.2

Carrivick, J.L., Smith, M.W., Quincey, D.J., 2016. Structure from Motion in the Geosciences. Collection of New Analytical Methods in Earth Environmental Sciences. DOI: https://10.1002/9781118895818

Cawood, A.J., Bond, C.E., 2019. eRock: An open-access repository of virtual outcrops for geoscience education. GSA Today, 29, 36-37.

Corradetti, A., Seers, T., Mercuri, M., Calligaris, C., Busetti, A., Zini, L., 2022. Benchmarking different SfM-MVS photogrammetric and iOS LiDAR acquisition methods for the digital preservation of a short-lived excavation: a case study from an area of sinkhole related subsidence. Remote Sensing, 14(20), 5187. DOI: https://doi.org/10.3390/rs14205187

Corradini, C., Suttner, T.J. (eds.), 2015. The Pre-Variscan sequence of the Carnic Alps (Austria and Italy). Abhandlungen der Geologisches Bundesantsalt, 69, 158pp. ISBN 978-3-85316-081-7

Corradini, C., Pondrelli, M., 2021. The Pre-Variscan Sequence of the Carnic Alps (Italy and Austria). Geological Field Trips and Maps, 13(2.1), 71pp. DOI: https://doi.org/10.3301/GFT.2021.05

Corradini, C., Corriga, M.G., Männik, P., Schönlaub, H.P., 2015a. Revised conodont stratigraphy of the Cellon section

(Silurian, Carnic Alps). Lethaia, 48, 56-71. DOI: https://doi.org/10.1111/let.12087

Corradini, C., Suttner, T.J., Ferretti, A., Pohler, S.M.L., Pondrelli, M., Schönlaub, H.P., Spalletta, C., Venturini, C., 2015b. The Pre-Variscan sequence of the Carnic Alps - an introduction. In: Corradini, C., Suttner, T., (eds.), The Pre-Variscan sequence of the Carnic Alps (Austria and Italy). Abhandlungen der Geologisches Bundesantsalt, 69, 7-15.

Corradini, C., Spalletta, C., Mossoni, A., Matyja, H., Over, D.J., 2017a. Conodonts across the Devonian/Carboniferous boundary: a review and implication for the redefinition of the boundary and proposal of an updated conodont zonation. Geological Magazine, 154, 888-902. DOI: https://doi.org/10.1017/S001675681600039X

Corradini, C., Mossoni, A., Pondrelli, M., Simonetto, L., Spalletta, C., Zucchini, R., 2017b. Sub-aerial exposures in the Tournaisian (Lower Carboniferous) of the central Carnic Alps (Italy). Stratigraphy, 14, 87-96. DOI: https://doi.org/10.29041/strat.14.1-4.87-96

Corradini, C., Corriga, M.G., Pondrelli, M., Spina, A., Suttner, T.J., 2024a. The "Lochkovian-Pragian Event" re-assessed: new data from the low latitude shelf of peri-Gondwana. Palaeogeography, Palaeoclimatology, Palaeoecology, 656, 112580. DOI: https://doi.org/10.1016/palaeo.2024.112580

Corradini, C., Henderson, C., Barrick, J.E., Ferretti, A., 2024b. Conodonts in biostratigraphy. A 300-million-years long journey through geological time. Newsletters on stratigraphy, 40pp. DOI: https://doi.org/11.1127/nos/2024/0822

Corriga, M.G., Corradini, C., Schönlaub, H.P., Pondrelli, M., 2016. Lower Lochkovian (Lower Devonian) conodonts from Cellon section (Carnic Alps, Austria). Bulletin of Geosciences, 91, 261-270. DOI: https://doi.org/10.3140/bull.geosci.1594

Corriga, M.G., Corradini, C., Pondrelli, M., Schönlaub, H.P., Nozzi, L., Todesco, R., Ferretti, A., 2021. Uppermost Ordovician to lowermost Devonian conodonts from the Valentintörl section and comments on the post Hirnantian hiatus in the Carnic Alps. Newsletters on Stratigraphy, 54, 183-207. DOI: https://doi.org/10.1127/nos/2020/0614

Devuyst, F.X., Kalvoda, J., 2007. Early evolution of the genus *Eoparastaffella* (Foraminifera) in Eurasia: the 'interiecta group' and related forms, late Tournaisian to early Viséan (Mississippian). Journal of Foraminiferal Research, 37, 69-89.

Devuyst, F.X., Hance, L., Hou, H., Wu, X., Tian, S., Coen, M., Sevastopulo, G., 2003. A proposed Global Stratotype Section and Point for the base of the Visean Stage (Carboniferous): the Pengchong section, Guangxi, South China. Episodes, 26, 105-115.

El Kabouri, J., Errami, E., Becker-Krber, B., Ennih, N., Youbi, N., 2023. Microbially induced sedimentary structures from the Ediacaran of Anti-Atlas, Morocco. Precambrian Research, 395, 107135. DOI: https://doi.org/10.1016/j.precamres.2023.107135

Farabegoli, E., Perri, M.C., Spalletta, C., Joachimski, M.M., Andrew, A., Pondrelli, M., 2023. Physical and biological events across the Frasnian-Famennian boundary (Late Devonian) in continuous oxic carbonate successions in the western Thetys (Carnic Alps of Italy and Austria). Bollettino della Società Paleontologica Italiana, 62, 143-217. DOI: https://doi.org/10.4435/BSPI.2023.06

Favalli, M., Fornaciai, A., Isola, I., Tarquini, S., Nannipieri, L., 2012. Multiview 3D reconstruction in geosciences. Computer & Geosciences, 44, 168-176. DOI: https://doi.org/10.1016/j.cageo.2011.09.012

Gedik, I., 1974. Conodonten aus dem Unterkarbon der Karnischen Alpen. Abhandlungen der Geologischen Bundesanstalt, 31, 1-43.

Groessens, G., 1974. Distribution des conodontes dans le Dinantien de la Belgique. In: Bouckaert, J. and Streel, M., Eds., International Symposium on Belgium micropaleontological Limits from Emsian to Visean. Brussels: Geological Survey of Belgium, Publication, 17, 1-193.

Hance, L., Muchez, P., Hou, H.F., Wu, X., 1997. Biostratigraphy, sedimentology and sequence stratigraphy of the Tournaisian-Viséan transitional strata in South China (Guangxi). Geological Journal, 32, 337-337.

Hance, L., Poty, E., Devuyst, F.X., 2001. Stratigraphie séquentielle du Dinantien type (Belgique) et corrélation avec le Nord de la France (Boulonnais, Avesnois). Bulletin de la Société géologique de France, 172, 411-426.

Herbig, H.-G., 2016. Mississippian (Early Carboniferous) sequence stratigraphy of the Rhenish Kulm Basin, Germany. Geologica Belgica, 19, 81-110. DOI: https://doi.org/10.20341/gb.2016.010

Higgins, A.C., Austin, R.L., 1985. A stratigraphical index of Conodonts. Chichester, British Micropalaeontological Society, Ellis Herwood Limited, 263pp.

Joachimski, M.M., Buggisch, W., Anders, T., 1994. Mikrofazies, Conodontenstratigraphie und Isotopengeochemie des Frasne-Famenne-Grenzprofils Wolayer Gletscher (Karnische Alpen). Abhandlungen der Geologischen Bundesanstalt, 50, 183-195.

Kaiser, S.I., Becker, R.T., Spalletta, C., Steuber, T., 2009. High-resolution conodont stratigraphy, biofacies and extinctions around the Hangenberg Event in pelagic successions from Austria, Italy and France. Palaeontographica Americana, 63, 97-139.

Lane, H.R., Ziegler, W., 1983. Taxonomy and phylogeny of *Scaliognathus* Branson and Mehl 1941 (Conodonta, Lower Carboniferous). Senkenbergiana lethaea, 64, 199-225.

Lane, H.R., Sandberg, C.A., Ziegler, W., 1980. Taxonomy and phylogeny of some Lower Carboniferous conodonts and preliminary standard post-*Siphonodella* zonation. Geologica et Palaeontologica, 14, 117-164.

Liu, B., Qi, Y., Wang, M., He, W., Du, Y., Li, D., & Dai, M., 2024. Thalassinoides ichnofabrics from the Zhangxia Formation (Cambiran Miaolingian series) in Henan province: Bioturbators as Ecosystem engineers. Palaeogeography, Palaeoclimatology, Palaeoecology, 640, 112103. DOI: https://doi.org/10.1016/j.palaeo.2024.112103

Mehl, M.G., Thomas, L.A., 1947. Conodonts from the Fern Glen of Missouri. Denison University Bulletin, Journal of the Science Laboratory, 40, 3-20.

Nemyrovska, T.I., Perret-Mirouse, M.-F., Weyant, M., 2006. The early Visean (Carboniferous) conodonts from the Saoura Valley, Algeria. Acta Geologica Polonica, 56, 361-370.

Perret, M.F., Devolve, J.J., 1994. Répartition vertical des conodontes carboniferes des region Pirénéennes; un commentaire. Memoires Institut Géologique de l'Université Catholique de Louvain, 35, 197-203.

Perri, M.C., Spalletta, C., 1998a. The Upper *marginifera* Zone (Late Devonian) in the Casera Collinetta di Sotto C section (Carnic Alps, Italy). In: Perri, M.C., Spalletta, C. (eds.). Southern Alps Field Trip Guidebook, ECOS VII. Giornale di Geologia, 60 Special Issue, 150-157.

Perri, M.C., Spalletta, C., 1998b. Late Famennian conodonts from the Casera Collinetta di Sotto B section (Carnic Alps, Italy). In: Perri, M.C., Spalletta, C. (eds.). Southern Alps Field Trip Guidebook, ECOS VII. Giornale di Geologia, 60 Special Issue, 158-167.

Perri, M.C., Spalletta, C., 1998c. Latest Devonian and Early Carboniferous conodonts from the Casera Collinetta di Sotto A section (Carnic Alps, Italy). In: Perri, M.C., Spalletta, C. (eds.). Southern Alps Field Trip Guidebook, ECOS VII. Giornale di Geologia, 60 Special Issue, 168-181.

Perri, M.C., Spalletta, C., 1998d. Conodont distribution at the Tournaisian/Viséan boundary in the Carnic Alps (southern Alps, Italy). Palaeontologia Polonica, 58, 225-245.

Pondrelli, M., Corradini, C., Corriga, M.G., Kido, E., Mossoni, A., Simonetto, L., Spalletta, C., Suttner, T., Carta, N., 2015. Depositional and deformational evolution of a Lower Paleozoic portion of the Southalpine domain: the Mt. Pizzul area (Carnic Alps, Italy). International Journal of Earth Sciences, 104, 147-178. DOI: https://doi.org/10.1007/s00531-014-1069-7

Pondrelli, M., Corradini, C., Spalletta, C., Suttner, T.J., Simonetto, L., Perri, M.C., Corriga, M.G., Venturini, C., Schönlaub, H.P., 2020. Geological map and stratigraphic evolution of the central sector of the Carnic Alps (Austria-Italy). Italian Journal of Geosciences, 139, 469-484. DOI: https://doi.org/10.3301/IJG.2020.16

Poty, E., 2016. The Dinantian (Mississippian) succession of southern Belgium and surrounding areas: stratigraphy improvement and inferred climate reconstruction. Geologica Belgica, 19, 177-200. DOI: https://doi.org/10.20341/gb.2016.014

Pratt, B.R., 1998. Syneresis cracks: subaqueous shrinkage in argillaceous sediments caused by earthquake-induced dewatering. Sedimentary Geology, 117, 1-10. DOI: https://doi.org/10.1016/s0037-0738(98)00023-2

Pratt, B.R., Ponce, J.J., 2019. Sedimentation, earthquakes, and tsunamis in a shallow, muddy epeiric sea: Grinnell Formation (Belt Supergroup, ca. 1.45 Ga), western North America. GSA Bulletin, 131, 1411-1439. DOI: https://doi.org/10.1130/b35012.1

Pratt, B.R., Hopkins, G.J., Hopkins, R.J., 2024. Bellerophontid molluscs in the Grimsby Formation (Llandovery, lower Silurian), Hamilton, Ontario, Canada and their paleoecological and taphonomic implications. Canadian Journal of Earth Sciences, 61, 833-842. DOI: https://doi.org/10.1139/cjes-2023-0146

Qie, W., Algeo, T.J., Luo, G., Herrmann, A., 2019. Global events of the Late Paleozoic (Early Devonian to Middle Permian): A review. Palaeogeography, Palaeoclimatology, Palaeoecology, 531, 109259. DOI: https://doi.org/10.1016/j.palaeo.2019.109259

Sandberg, C.A., Ziegler, W., Leuteritz, K., Brill, S.M., 1978. Phylogeny, speciation and zonation of Siphonodella (Conodonta, Upper Devonian and Lower Carboniferous). Newsletters on Stratigraphy, 7, 102-120.

Schönlaub, H.P., Feist, R., Korn, D., 1988. The Devonian-Carboniferous Boundary at the section "Grüne Schneid" (Carnic Alps), Austria: A preliminary report. Courier Forschungs-Institut Senckenberg, 100, 149-167.

Schönlaub, H.P., Klein, P., Magaritz, M., Rantitsch, G., Scharbert, S., 1991. Lower Carboniferous paleokarst in the Carnic Alps (Austria, Italy). Facies, 25, 91-117.

Spalletta, C., Venturini, C., 1988. Conglomeratic Sequences in the Hochwipfel Formation: a new palaeogeographic hypothesis on the Hercynian Flysch Stage of the Carnic Alps. Jahrbuch der Geologischen Bundesanstalt, 131, 637-647.

Spalletta, C., Venturini, C., 1995. Late Devonian-Early Carboniferous synsedimentary tectonic evolution of the Palaeocarnic domain (Southern Alps, Italy). Giornale di Geologia, 56, 211-222

Spalletta, C., Perri, M.C., Pondrelli, M., Corradini, C., Mossoni, A., Schönlaub, H.P., 2015a. Pal Grande Formation. In: Corradini, C., Suttner, T.J. (eds.). The Pre-Variscan sequence of the Carnic Alps (Austria and Italy). Abhandlungen der Geologisches Bundesantsalt, 69, 137-140.

Spalletta, C., Schönlaub, H.P., Pondrelli, M., Corradini, C., Simonetto, L., 2015b. Plotta Formation. In: Corradini, C., Suttner, T.J. (eds.). The Pre-Variscan sequence of the Carnic Alps (Austria and Italy). Abhandlungen der Geologisches Bundesantsalt, 69, 145-147.

Spalletta, C., Corradini, C., Feist, R., Korn, D., Kumpan, T., Perri, M.C., Pondrelli, M., Venturini, C., 2021. The Devonian/Carboniferous Boundary in the Carnic Alps (Austria and Italy). Palaeobiogeography and Palaeoenvironments, 101, 487-505. DOI: https://doi.org/10.1007/s12549-019-00413-3

Thompson, T.L., Fellows, L.D., 1970. Stratigraphy and conodont biostratigraphy of Kinderhookian and Osagean (Lower Mississippian) rocks of southwestern Missouri and adjacent areas. Rolla, Missouri Geological Survey and Water Resources. Report of Investigations, 45, 263pp.

Vai, G.B., 1998. Field trip through the Southern Alps: an introduction with geologic settings, palaeogeography and Palaeozoic stratigraphy. In: Perri, M.C., Spalletta, C. (eds.). Southern Alps Field Trip Guidebook, ECOS VII. Giornale di Geologia, 60 Special Issue, 1-38.

Venturini, C., Spalletta, C., 1998. Remarks on the Palaeozoic stratigraphy and the Hercynian tectonics of the Palaeocarnic chain (Southern Alps). In: Perri, M.C., Spalletta, C. (eds.).

Southern Alps Field Trip Guidebook, ECOS VII. Giornale di Geologia, 60 Special Issue, 69-88.

Von Raumer, J.F., Stampfli, G.M., Borel, G., Bussy, F., 2002. Organization of pre-Variscan basement areas at the north-Gondwanan margin. International Journal of Earth Sciences, 91, 35-52.

Voges, A., 1959. Conodonten aus dem Unterkarbon I and II (Gattendorfia und Pericyclus-Stufe) des Sauerlandes. Paläontologische Zeitschrift, 3, 266-314.

Walliser, O.H., 1964. Conodonten des Silurs. Abhandlungen hessisches Landesamt für Bodenforschung, 41, 1-106.

Xu, X., Aiken, C.L., Bhattacharya, J.P., Corbeanu, R.M., Nielsen, K.C., McMechan, G.A., Abdelsalam, M.G., 2000. Creating virtual 3-D outcrop. Lead. Edge, 19, 197-202. DOI: https://doi.org/10.1190/1.1438576

Yanin, B.T., Baraboshkin, E.Y., 2013. Thalassinoides burrows (decapoda dwelling structures) in lower cretaceous sections of southwestern and central Crimea. Stratigraphy and Geological Correlation, 21(3), 280-290. DOI: https://doi.org/10.1134/s086959381303009x

Ziegler, W., 1960. Die Conodonten aus den Gerollen des Zechsteinconglomerate von Rossensay (sudwestlich Rheinberg/Niederrhein). Fortschritte in der Geologie von Rheinland and Westfalen, 6, 1-15.

Ziegler, W., Lane, H.R., 1987. Cycles in conodont evolution from Devonian to mid-Carboniferous. In: Aldridge R.J. (ed.). Palaeobiology of Conodonts, British Micropalaeontological Society, Ellis Herwood Limited, 147-163.

Zocchi, C., 2022. Datazione di un livello di mud crack del Carbonifero inferiore nelle Alpi Carniche. Bachelor Thesis, Università di Trieste, 41pp.

Zocchi, C., Corradini, C., 2024. Tecnica fotomicrografica innovativa per riprese di microfossili. In: Bianucci, G., Merella, M., Collareta, A. (eds.). XXIV Edition of the "Giornate di Paleontologia". Pisa, (4) 5-7 June 2024 abstract book, 116.

Manuscript received December 2024;
revision accepted April 2025;
published Online July 2025.